Article

Current Biology

Adaptation of Inhibition Mediates Retinal Sensitization

Highlights

- Tonic inhibitory amacrine transmission decreases during sensitization
- Inhibition from sustained amacrine cells can reproduce or cancel sensitization
- Replaying the visual response of a single amacrine cell can trigger sensitization
- Sensitization is reproduced by a model of inhibitory synaptic depression

Authors

David B. Kastner, Yusuf Ozuysal, Georgia Panagiotakos, Stephen A. Baccus

Correspondence

baccus@stanford.edu

In Brief

Retinal sensitization is a form of short-term plasticity that elevates local sensitivity after strong visual stimulation. Kastner et al. show that sensitization is mediated by adaptation of inhibitory amacrine cells. Adaptation of inhibition is a general mechanism to enhance sensitivity to specific sensory features and to predict future input.

Kastner et al., 2019, Current Biology *29*, 2640–2651
August 19, 2019
https://doi.org/10.1016/j.cub.2019.06.081

CellPress

CellPress

Current Biology
Article

Adaptation of Inhibition Mediates Retinal Sensitization

David B. Kastner,[1,4] Yusuf Ozuysal,[2,5] Georgia Panagiotakos,[1,6] and Stephen A. Baccus[3,7,*]
[1]Neuroscience Program, Stanford University School of Medicine, 299 Campus Drive W., Stanford, CA 94305, USA
[2]Department of Electrical Engineering, Stanford University School of Medicine, 299 Campus Drive W., Stanford, CA 94305, USA
[3]Department of Neurobiology, Stanford University School of Medicine, 299 Campus Drive W., Stanford, CA 94305, USA
[4]Present address: Department of Psychiatry, University of California, San Francisco, 401 Parnassus Avenue, San Francisco, CA 94143, USA
[5]Present address: Google Inc., Mountain View, CA 94043, USA
[6]Present address: Broad Center of Regeneration Medicine and Stem Cell Research, University of California, San Francisco, 35 Medical Center Way, San Francisco, CA 94143, USA
[7]Lead Contact
*Correspondence: baccus@stanford.edu
https://doi.org/10.1016/j.cub.2019.06.081

SUMMARY

In response to a changing sensory environment, sensory systems adjust their neural code for a number of purposes, including an enhanced sensitivity for novel stimuli, prediction of sensory features, and the maintenance of sensitivity. Retinal sensitization is a form of short-term plasticity that elevates local sensitivity following strong, local, visual stimulation and has been shown to create a prediction of the presence of a nearby localized object. The neural mechanism that generates this elevation in sensitivity remains unknown. Using simultaneous intracellular and multielectrode recording in the salamander retina, we show that a decrease in tonic amacrine transmission is necessary for and is correlated spatially and temporally with ganglion cell sensitization. Furthermore, introducing a decrease in amacrine transmission is sufficient to sensitize nearby ganglion cells. A computational model accounting for adaptive dynamics and nonlinear pathways confirms a decrease in steady inhibitory transmission can cause sensitization. Adaptation of inhibition enhances the sensitivity to the sensory feature conveyed by an inhibitory pathway, creating a prediction of future input.

INTRODUCTION

Understanding how individual components of a neural circuit cause a biological function presents a challenging problem. Within a neural circuit, signals travel through serial connections and parallel pathways through a diversity of cell types. The components of those circuits often have nonlinear and interdependent effects, meaning that the effects of individual mechanisms must be considered in the context of a particular computation. Consequently, the mechanisms of even well-studied neural computations, such as the receptive fields of orientation selective neurons in the primary visual cortex [1, 2], remain incompletely understood.

Circuit computations—those that arise not by the action of a single cell but by the interaction of multiple neurons in a circuit—present a particularly difficult challenge for mechanistic inquiry because of the need to study the intact circuit. Yet circuit computations also provide an opportunity for understanding because of the ability to perturb neurons in the circuit as it operates. One such circuit computation is retinal sensitization, a process seen in multiple species that elevates local sensitivity following strong local stimulation [3–5]. Slow contrast adaptation is a process that changes the threshold over a timescale of seconds, causing cells to become less sensitive in a high-contrast environment, where stimulus contrast is defined as the SD of intensity divided by the mean. At the transition to low contrast, cells showing adaptation exhibit a lowered firing rate and elevated threshold, which then increases as cells lower their threshold in the low-contrast environment. Contrast sensitization has an opposing time course to contrast adaptation and can be observed after the transition from a high-contrast stimulus to low contrast as an increase in firing and a lowered threshold (Figure 1A). Theoretical analyses and experiments have indicated that this elevation of sensitivity during sensitization embodies a prediction that a target stimulus feature will be present in the future in that same region [5]. The prediction of future sensory input is an important overall function of the nervous system [6, 7], yet the mechanisms of such computations are generally unknown.

Previous computational and experimental work has proposed that high contrast stimulates amacrine cells, causing them to adapt, and that this adaptation persists during low contrast to cause sensitization [3–5]. As evidence for this proposal, transmission from GABAergic amacrine cells is required for sensitization [4, 5], raising the possibility that GABAergic inhibition could mediate sensitization. However, it might also be that GABAergic inhibition is a modulator of sensitization rather than a mediator [8] or that the slow action of pharmacological manipulations causes compensatory actions in the retina, taking the circuit out of the operating range where sensitization can occur [9].

Here, we use simultaneous intracellular and multielectrode recording in the salamander retina to establish quantitatively the causal role of a class of inhibitory interneurons in the computation of sensitization. We take the approach of measuring the responses of an interneuron and how its transmission affects

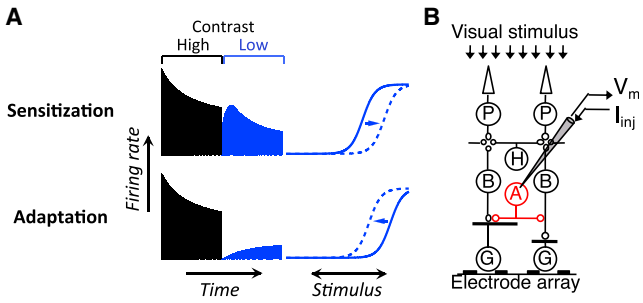

Figure 1. Sensitization, Adaptation, and Experimental Setup

(A) Schematic depiction of contrast sensitization and adaptation. Left: firing rate of typical ganglion cells showing contrast sensitization (top) or adaptation (bottom), based on fits to data from [3]. After the transition from high to low contrast, sensitization and adaptation exhibit opposite dynamics during low contrast (blue). During sensitization, high contrast elevates firing at the beginning of low contrast, and then activity decreases during low contrast. During adaptation, high contrast causes decreased firing at the transition from high to low contrast, and activity recovers during low contrast. For sensitization, underlying this increase in firing rate is a lowered threshold of the ganglion cell response curve (right), which then recovers over a period of seconds. Underlying slow contrast adaptation is an increased threshold, which then recovers.

(B) Experimental setup for simultaneous intracellular and multielectrode recording.

the output of the circuit. Note that "transmission" in the context of this experiment includes both monosynaptic and polysynaptic transmission, and connections are not assumed to be monosynaptic. We find that the output from sustained amacrine cells decreases during sensitization caused by a localized stimulus. In addition, we observe a separate effect of a smaller hyperpolarization in the response of these amacrine cells during sensitization. Using current injection, we show that changing amacrine cell inhibitory transmission can reproduce or cancel sensitization in ganglion cells. We further use current injection to replay the visual input experienced by an individual amacrine cell, finding that this input is sufficient to induce subsequent sensitization in ganglion cells. Finally, a computational model characterizes the change in steady inhibitory transmission and shows that it accounts quantitatively for the observed sensitivity changes. We conclude that a decrease in transmission in two stages of an inhibitory pathway mediates sensitization.

Behavioral sensitization has been attributed to changes in excitatory synaptic strength or intrinsic excitability [10]. At the circuit level, adaptation of excitation allows a cell to maintain sensitivity to the cell's primary input [11, 12] and can underlie the subtraction of a prediction by diminishing the expected result of the circuit and thereby transmitting a signal enriched for novelty [13–17]. In contrast, we find that adaptation of an inhibitory pathway provides a general mechanism for the presence of a sensory feature to subsequently cause an enhanced sensitivity for that feature, creating a prediction of future input.

RESULTS

GABAergic transmission is necessary for the short-term plasticity of sensitization in the salamander and zebrafish retina, and a decrease in amacrine synaptic release occurs during sensitization [4, 5]. However, these previous results cannot distinguish between the requirement for only a constant level of inhibition and a dynamic change in the level of inhibitory neurotransmission. Furthermore, such results do not show that a change in inhibition has a causal effect, being sufficient to reproduce sensitization.

For a number of reasons, we focused on sustained Off-type amacrine cells, which are GABAergic, and comprise at least two types [18]. In the salamander retina, sensitization persists when the On pathway is blocked, making On-type amacrine cells an unlikely candidate [5]. A model that reproduces sensitization contains an inhibitory pathway with a tonic output that increases sensitivity during sensitization through disinhibition [3, 5], and sustained Off amacrine cells have been shown to function largely through disinhibition [19]. Finally, sensitization occurs at a scale smaller than the ganglion cell receptive field center [3, 5], making it less likely that the inhibitory cell will have a large receptive or projective field. Sustained Off amacrine cells are narrow field, having small receptive and projective fields [20], especially when compared to transient cells like the polyaxonal amacrine cell [21, 22].

A Sensitizing Stimulus Creates an Afterhyperpolarization in Amacrine Cells

As the retina processes signals from photoreceptors to ganglion cells, the effect of a particular interneuron, such as an amacrine cell, can be logically divided into two stages: (1) the input to the amacrine cell, consisting of the circuitry that leads from photoreceptors to bipolar cells to the amacrine cell membrane potential, and (2) the output from the amacrine cell, comprising the circuitry that leads from the amacrine cell membrane potential to the ganglion cell. These two stages may partially overlap to the extent that the membrane potential influences feedback mechanisms, such as spike-dependent conductances. Understanding the contribution of an interneuron to the processing of the entire circuit requires measurement of both the membrane potential response of the neuron—reflecting the input stage—and the effects of its output on the circuit [23].

We first sought to determine whether the first stage—the amacrine cell input stage—exhibited any change in processing that was correlated with the dynamics of sensitization. To do this, we simultaneously recorded intracellularly from a sustained Off-type amacrine cell and extracellularly from multiple nearby ganglion cells (Figures 1B and 2A), all while presenting to the retina a visual stimulus that causes sensitization by alternating between high (4 s) and low temporal contrast (16 s; Figures 2C and 2D). Ganglion cell sensitization, as previously described [3, 5], is observed as an elevated firing rate after the transition to low contrast that decays to a lower level during low contrast. We analyzed fast Off-type adapting and sensitizing ganglion cells, two salamander cell types that form independent mosaics across the retina [3]. Both cell types sensitize (Figure S1C), although adapting fast Off cells have stronger adaptation in the receptive field center that cancels some sensitization [5]. In some cases, we observed a slow increase in firing during high contrast (Figure 2C), which is consistent with the model that sensitization in ganglion cells is caused by adaptation by amacrine cells during high contrast that persists during low contrast [5]. The analysis of this study, however, concentrated on low

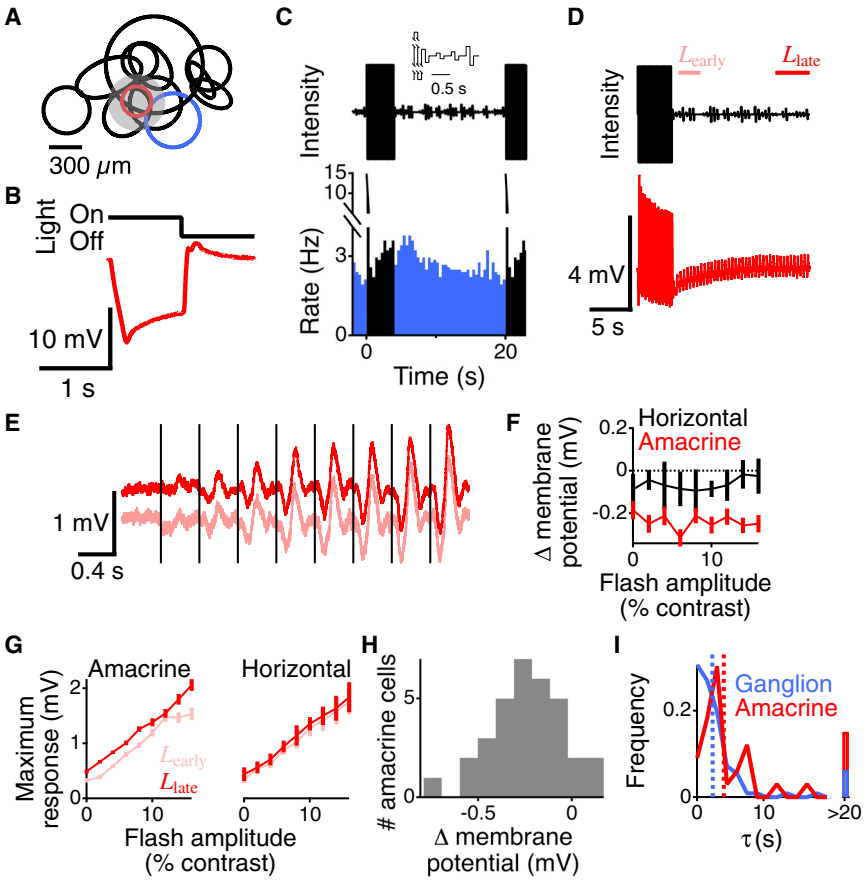

Figure 2. Amacrine Cells Hyperpolarize after a Sensitizing Stimulus

(A) Spatial receptive fields of an amacrine cell (red) and ganglion cells (black and blue) recorded simultaneously. Gray shaded region shows the localized spot that flickered at high contrast to generate sensitization.

(B) Average response of a sustained Off amacrine cell to a 0.5-Hz flashing stimulus.

(C) Visual stimulus (top) and the response (bottom) of an example ganglion cell (blue receptive field from A) showing sensitization as an elevated response to low contrast (colored trace) following high contrast. Flashes were biphasic, consisting of 0.1 s of an intensity $+I$ greater than the mean followed by 0.1 s of an intensity $-I$ less than the mean, followed by 0.2 s of the mean intensity (inset). High contrast was 100% Michelson contrast, and low contrast ranged from 0% to 16% contrast chosen randomly every 0.4 s. The high contrast was only presented over the receptive field of the amacrine cell, and the rest of the image was uniform field low contrast. Firing rates are averaged over presentations of many different sequences. In each sequence, peak firing rates exceed 100 Hz, but because of long periods of silence, averaging over different sequences yields a much lower average rate [24].

(D) Visual stimulus (top) and the response of an example amacrine cell (bottom, red receptive field from (A), which became rectified at high contrast as indicated by larger depolarizing fluctuations.

(E) Average membrane potential of the amacrine cell shown in (B) to the nine different low-contrast flashes. Time intervals for L_{early} and L_{late} are shown above the stimulus in (D), and although the different flashes were randomly interleaved, they are shown here concatenated in order of increasing strength, with vertical lines demarcating the different flashes.

(F) Maximum depolarization in response to a flash as a function of flash amplitude for amacrine (n = 33) and horizontal (n = 4) cells during L_{early} and L_{late}.

(G) Average difference in the membrane potential across the duration of the flash for each flash amplitude between L_{late} and L_{early} for amacrine (n = 33, red) and horizontal (n = 4, black) cells. Negative values indicate that the cell was more hyperpolarized during L_{early} compared to L_{late}. Error bars in (F) and (G) indicate SEM.

(H) Histogram of the average hyperpolarization during L_{early} for the population of amacrine cells.

(I) Histogram of the time constant of an exponential fit to amacrine cell recovery from hyperpolarization and to ganglion cell sensitization. Vertical dashed line indicates the median for each distribution.

See also Figure S1.

contrast. We quantified the amount of sensitization using an adaptation index, defined as $A = (r_{early} + r_{late}/r_{early} + r_{late})$, where r_{early} and r_{late} are the average rate of the ganglion cell during the time intervals L_{early} (0.8–3.2 s after the transition to low contrast) and L_{late} (12–16 s after the transition), respectively. Although sensitization had not completely reached baseline at 16 s, this time interval was sufficient to measure the difference in firing rate caused by sensitization between L_{early} and L_{late}.

We tested whether individual sustained Off amacrine cells (Figure 2B), which in the salamander are GABAergic [25], changed their response properties to a localized flashing spot stimulus that sensitizes ganglion cells. To localize the effect to the single amacrine cell we were manipulating, we created an online map of the receptive field of the amacrine cell (Figure 2A) using a white-noise checkerboard stimulus. This allowed us to place a flickering high-contrast spot over the amacrine cell and then measure its membrane potential when the spot changed from high to low contrast (Figure 2D). High contrast was 100% Michelson contrast, defined as $(I_{max} - I_{min})/(I_{max} + I_{min})$, and low contrast was composed of 200-ms biphasic flashes of 9 different amplitudes randomly interleaved. Such a localized high contrast also sensitizes more ganglion cells than does a uniform field stimulus because of the center-surround spatial antagonism of adaptation and sensitization [5].

Sustained Off amacrine cells showed a dynamic response that correlated with the time course of sensitization—they adapted to the contrast of the focal stimulus by hyperpolarizing during sensitization (Figures 2D–2G). Their membrane potential hyperpolarized immediately after the transition from a high to a low contrast, L_{early}, compared to later during low contrast, L_{late}. This hyperpolarization was similar to an afterhyperpolarization seen in ganglion cells and cortical neurons undergoing contrast adaptation [26, 27] and in some amacrine cells during contrast adaptation [24]. The magnitude of this hyperpolarization during L_{early} was -0.24 ± 0.3 mV, with a range of -0.79 to 0.17 (n = 33; Figure 2H). Although the size of this hyperpolarization appears small, its potential effects are discussed below in relationship to a computational model of sensitization (Figure 6). This hyperpolarization occurred across all flash values

(Figure 2G), amounting to a steady change in membrane potential without a change in gain.

Amacrine cells recovered from their hyperpolarization with a median time course of 4.0 s, which was similar to the median time course of recovery of sensitization in ganglion cells (2.4 s). Ganglion cells and amacrine cells also showed a similar range of values (Figure 2I). The slightly more prolonged time course of amacrine cell hyperpolarization is explained below by the model of sensitization (Figure 6).

Although sustained Off amacrine cells do not adapt to uniform-field Gaussian stimuli [24], this stronger, more focal stimulus did generate adaptation. Additionally, we observed that the membrane potential response to the focal stimulus was more strongly rectified than for previous measurements to a full field stimulus, meaning that depolarizing fluctuations were larger than hyperpolarizing fluctuations (Figure 2D). This rectified response causes a change in the mean membrane potential at high contrast. A previously described accurate model of contrast adaptation indicates that a change in the mean signal level will cause adaptation, likely by causing synaptic depression in the bipolar cell inputs to the cell [11]. In contrast, horizontal cell responses were not rectified and did not hyperpolarize following high contrast (Figures 2F and 2G), indicating that they do not adapt to contrast, consistent with previous observations [24].

Sustained Amacrine Cells Deliver Tonic Inhibition to Nearby Ganglion Cells that Decreases during Sensitization

Having found that amacrine cells changed their membrane potential in response to a sensitizing stimulus, we next tested whether, during sensitization, there were changes in the transmission from the amacrine cell—the amacrine cell output stage, which is the stage between the interneuron and ganglion cells. If amacrine cell transmission contributed to sensitization, one would expect it to decrease during L_{early} relative to L_{late}. To test whether amacrine transmission changed during sensitization, we first measured the firing rate of the ganglion cell as a function of the amplitude of a flash of light; this is the ganglion cell light response curve. Then we measured how this response function changed when we delivered either depolarizing or hyperpolarizing pulses (±500 pA) to the amacrine cell (Figures 3A and 3B; STAR Methods). A −500-pA current hyperpolarized the membrane 13 ± 1 mV, with a time constant of 24 ± 5 ms (n = 11 amacrine cells; Figure S2). This is considerably smaller than the 24.5 ± 1.6 mV (n = 33 amacrine cells) average amplitude of a full field 100% contrast 0.5 Hz full-field stimulus and is thus within the physiological range of membrane potentials. Note that the aim was not to match the low-contrast visual response by current injection but to use the current as a probe to measure the gain of the synapse in the conditions of L_{early} and L_{late}.

The ganglion cell light response curve was approximately sigmoidal. Depolarizing the amacrine cell caused the ganglion cell response curve to shift to the right, such that a larger amplitude light stimulus was needed to achieve a given ganglion cell firing rate. Because amacrine cell current injection altered the ganglion cell light response curve, we sought to measure whether this effect was different during sensitization. Light responses were analyzed from ganglion cells within 200 μm of the amacrine cell. To measure how the effects of amacrine transmission changed during sensitization between L_{early} and L_{late}, we fit the ganglion cell response curve with a sigmoid and measured the difference in the amount that current injection shifted the parameter specifying the midpoint of the sigmoid in units of Michelson contrast of the light stimulus between L_{early} and L_{late} (Figure 3C). The effect of amacrine hyperpolarization was to shift the ganglion cell light response curve 1.74% ± 0.32% Michelson contrast units to the left during L_{early}, meaning that a smaller amplitude visual stimulus was needed to achieve the same ganglion cell response. However, during L_{late}, amacrine hyperpolarization shifted the ganglion cell response curve by 2.92% ± 0.47% Michelson contrast, indicating that amacrine transmission was 40% smaller during sensitization ($p = 0.003$; paired t test). The effect of amacrine depolarization (1.25 ± 0.28 during L_{early} and 1.36 ± 0.32 during L_{late}) was less than half of that of hyperpolarization, consistent with previous observations that sustained amacrine cells release a strong tonic inhibition and mainly act by hyperpolarization and disinhibition of ganglion cells [19]. Consequently, although the distribution of effects from depolarization appeared similar in shape to the effects from hyperpolarization (Figure 3C), the magnitude of the effect was smaller, reducing by 9%, and was thus more uncertain ($p = 0.64$; paired t test). Thus, it appeared from this simple analysis that the effect of amacrine transmission on the ganglion cell light response was smaller during L_{early} than L_{late}.

Importantly, tonic inhibition has been shown to be critical to the action of sustained Off amacrine cells, in that these cells deliver a strong amount of steady inhibition onto ganglion cells, even with zero-contrast visual input, and act primarily through hyperpolarization driven by visual input, thereby disinhibiting ganglion cell and increasing their firing [19, 20]. To support this steady release, the cells deliver a steady output in response to a steady input, evidenced by a monophasic transmission filter [19]. Therefore, a hyperpolarizing pulse to an amacrine cell causes ganglion cell firing, even in the absence of any changing visual stimulus (Figure 3D). Consistent with there being less transmission from the amacrine cell to the ganglion cell during L_{early}, there was less tonic inhibition during L_{early} than L_{late} for cell pairs within 200 μm of each other ($p = 8 \times 10^{-5}$; paired t test; n = 70 cell pairs, 25 amacrine cells), with the ganglion cell response to amacrine current decreasing by 46% during L_{early} compared to L_{late}. Within 150 μm, this decrease was 58% during L_{early} compared to L_{late}. Because of the known importance of tonic inhibition, this reduction in tonic inhibition is expected to decrease the threshold for activation of ganglion cells by a visual stimulus.

The above analyses support the role for sustained Off amacrine cells in sensitization, because it suggests that they have diminished transmission to ganglion cells that sensitize during L_{early}. However, a critical issue in identifying which neurons contribute to a computation in a parallel and nonlinear circuit is whether the effect of one pathway is incorrectly assigned to another. We therefore performed a further analysis to verify that the changing effect of amacrine current injection arose due to plasticity of the transmission of that cell, as opposed to being an apparent effect from unrelated plasticity elsewhere in the circuit.

To illustrate this potential ambiguity, consider a simple neuron *G* that sums two inputs, *a* and *b*, and then passes

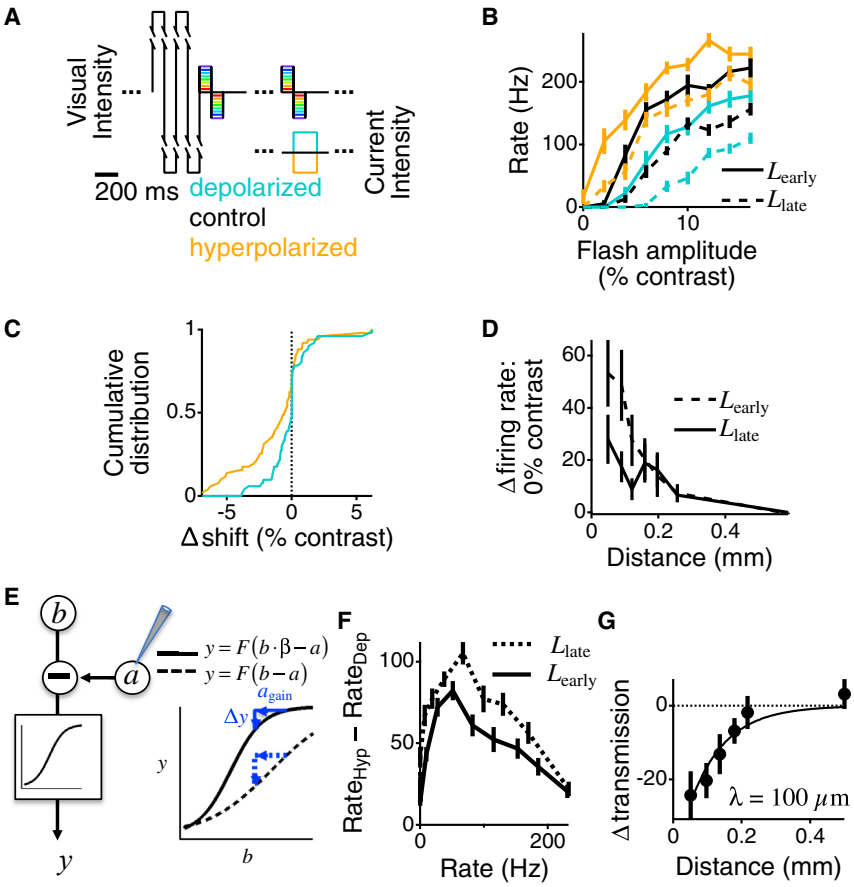

Figure 3. Amacrine Transmission Decreases during Sensitization

(A) Visual stimulus alternating between high and low contrast. High contrast was 100% Michelson contrast, presented only over the amacrine cell receptive field center, and low contrast, presented everywhere, was composed of flashes with nine different amplitudes randomly interleaved. Current pulses (±0.5 nA) were delivered for 200 ms, starting when the visual stimulus flash transitioned from light to dark. Current was only delivered during the flashes occurring during L_{early} and L_{late}, and all three conditions (hyperpolarizing current, depolarizing current, and control) were randomly interleaved at each stimulus presentation.

(B) Average response of an example ganglion cell to the nine different visual flashes during the six conditions of the experiment.

(C) Cumulative distribution of the difference in the shift of the ganglion cell response curve in response to amacrine cell hyperpolarization (orange) and depolarization (teal) between L_{early} and L_{late} (n = 51 cell pairs, 23 amacrine cells). Negative values indicate a smaller shift during L_{early} compared to L_{late}. The shift was computed as the change in the parameter μ that captured the effect of current injection on the ganglion cell light response curve, in units of Michelson contrast. Amacrine-ganglion cell pairs within 200 μm of each other whose response varied during hyperpolarizing current injection were included in the analysis.

(D) Change in the firing rate of the ganglion cell with no visual input in response to a −500-pA amacrine cell pulse, during L_{late} and L_{early}, plotted as a function of distance between the amacrine and ganglion cell (n = 107 cell pairs, 26 amacrine cells).

(E) Left: schematic diagram of an excitatory cell *b* and an inhibitory cell *a* that acts prior to a nonlinear function *F*() and is under direct experimental manipulation. (Right) Diagram of the output of the system in two conditions, when the gain β of *b* is high (solid line) and when the gain is low (dotted line) is shown. In this example, the output neuron *a* causes an effect Δ*y* when it is perturbed. In the two conditions, even though the gain of *a* is unchanged, it has a different effect because the resting condition is at a different point of the response curve.

(F) Average difference in the ganglion cell response $G(s)$ between the conditions of amacrine cell hyperpolarization ($Rate_{Hyp}$) and amacrine depolarization ($Rate_{Dep}$) as a function of the response of the ganglion cell, $\Delta G_A(G)$. Results are from all amacrine-ganglion cell pairs within 200 μm of each other (n = 60 cell pairs, 24 amacrine cells).

(G) Change in transmission as a function of distance between the amacrine and ganglion cell, averaged across all pairs (n = 95 cell pairs, 26 amacrine cells). The change in transmission is defined as the average difference between the effect of current on the ganglion cell firing rate as a function of the particular ganglion cell firing rate during control conditions ($\Delta G_A(G)_{early} - \Delta G_A(G)_{late}$) for each cell pair. A negative change in transmission indicates diminished transmission during L_{early} compared to L_{late}.

Error bars in (B), (C), (F), and (G) indicate SEM. See also Figure S2.

the sum through a sigmoidal input/output curve $N()$, such that $G = N(b + a)$ (Figure 3D). When perturbing *a*, the change in output depends on the present operating point along the sigmoid. If the strength of input *b* doubles, such that now $G = N(2b + a)$, any perturbations of *a* will be delivered at a different operating point with a different slope. Thus, even though all changes in the circuit are due to the pathway involving neuron *b* and the gain at which *a* is integrated has not changed, *a* may still have a different apparent effect on neuron *G* because of the nonlinear combination of the output of neurons *a* and *b*.

To rule out this source of an apparent change in transmission, we examined the difference in the ganglion cell response between hyperpolarizing and depolarizing the amacrine cell, not as a function of different light levels but as a function of different ganglion cell firing rates. We found that the smaller change in ganglion cell firing rate during L_{early} (Figure 3C) occurred across all ganglion cell firing rates (Figure 3E). We assessed this effect statistically using a permutation test, repeating the analysis with response curves drawn randomly with replacement from either L_{early} or L_{late} ($p = 6 \times 10^{-7}$). Thus, the decrease in the effect of amacrine cell current L_{early} was not from the action of another neural pathway as illustrated in (Figure 3D) but rather reflects a change in transmission between L_{early} and L_{late} from sustained Off amacrine cells to ganglion cells.

The decrease in amacrine transmission during L_{early} decayed as a function of distance between amacrine and ganglion cells with a space constant of $\lambda = 100 \pm 20 \mu m$ (Figure 3F). This increase in transmission from L_{early} to L_{late} is consistent with a recovery from synaptic depression, a process that exists in

amacrine cells [28]. These results show that, given the nonlinear properties of the circuit, a small hyperpolarization in sustained Off amacrine cells and a substantial decrease in their transmission is correlated in time and space with sensitization. Furthermore, this inhibitory transmission has a strong tonic component, implying that steady inhibition decreases during sensitization.

Changes in Amacrine Output Can Reproduce or Cancel Sensitization

Previous work has shown pharmacologically that inhibition is necessary for sensitization [4, 5]. This finding, however, does not distinguish between a permissive role of inhibition, such as setting the baseline threshold of ganglion cells, and our hypothesis that changes in amacrine inhibition mediate sensitization. To test the causal effects of changes in amacrine transmission on sensitization, we analyzed whether the effect from current injection into amacrine cells was one that could cause the specific changes in the visual response curve of a sensitized ganglion cell and not simply a change in average firing rate. Although the 200-ms current pulses were not chosen here to directly match the light response of the amacrine cell, because of the measured tonic transmission from amacrine cells, we measured the nature of the effects of a change in that tonic component. For these analyses, we used the same data from Figures 2 and 3, where we presented a flashing visual stimulus to the retina that allowed for the rapid measurement of the ganglion cell response as a function of light intensity.

A change from one sigmoid to another can be accounted for by four parameters that capture: (1) a horizontal shifting of the curve along the light intensity axis; (2) a horizontal scaling, which causes a change in the slope of the curve without changing the maximum; (3) a vertical shift in the curve; and (4) a vertical scaling that changes the maximum response. However, we found that only two parameters were needed to capture 79.9% ± 3.2% (hyperpolarizing) and 82.3% ± 3.2% (depolarizing) of the effects of amacrine current injection. Those two parameters were μ, a horizontal shifting of the ganglion cell response curve along the light intensity axis, and v, a horizontal scaling along the light intensity axis (Figures S2A and S2B; STAR Methods). The fact that changes in the sigmoid along the horizontal axis largely capture sensitization is consistent with prior results showing that sensitization can be observed presynaptic to ganglion cells in bipolar cell terminals [4, 5], because such an effect is at the input to the sigmoidal function rather than the output.

To determine whether decreased Off amacrine cell output was sufficient to create sensitization, we assessed, for each cell pair, whether the effects of hyperpolarizing current injected into the amacrine cell were the same as the effects of sensitization. To capture the effects of either current, sensitization, or both, we fit transformations consisting of horizontal shifting and scaling parameters between response curves in different conditions. For a given ganglion cell response curve $G(s)$, the horizontal shifting parameter creates an offset in the value of s, thus shifting the response curve along the horizontal axis, and the scaling parameter scales the value of s, thus scaling the curve horizontally (see STAR Methods for additional details).

To quantify the effects of sensitization, we computed the transformation, T_{sens}, that changed the control ganglion cell response curve from L_{late} to L_{early}. Similarly, we computed a transformation T_{Hyp} that captured the effects of hyperpolarizing current on the response curve during L_{late}. To then determine whether the two effects were similar, that of sensitization as captured by T_{sens} and that of hyperpolarizing current as captured by T_{Hyp}, we tested whether a single transformation, T_{Both}, fit to simultaneously capture both effects could capture the data as well as the two transformations, T_{Sens} or T_{Hyp}, fit separately.

Because sensitization likely resulted from the effects of multiple amacrine cells, in fitting T_{Both}, we allowed the effects of hyperpolarization to be scaled in amplitude to account for the observation that the response curve change during sensitization was not identical in magnitude to the effect of hyperpolarizing current. To accomplish this scaling, we computed a single parameter, κ_-, to scale the effects of hyperpolarization (Figure 4A). More specifically, $T_{Both} = (\mu, \nu)$, with the parameter μ that shifted the response curve and parameter v that scaled the response curve, was fit to capture the effects of hyperpolarizing current during L_{late}, and simultaneously, κ_- was fit so that $\kappa_- T_{Both} = (\kappa_- \mu, \kappa_- \nu)$ best captured the effects of sensitization from L_{late} to L_{early}.

We found that scaling the effects of hyperpolarizing current using the single transformation $\kappa_- T_{Both}$ captured 90.5% ± 3.1% of the effect of sensitization as captured by the single transformation T_{Sens} fit only to sensitization (Figure 4C). Furthermore, the simultaneously fit transformation T_{Both} captured 98.4% ± 7.2% of the effects of current as captured by T_{Hyp} fit only to hyperpolarizing current injection (Figure 4C). Therefore, reducing amacrine cell transmission with current injection produced nearly the same type of effect on the ganglion cell light response as sensitization. The value of κ_- (Figure 4D) on average was 0.99 ± 0.19, meaning that, on average, for the cell pairs we recorded from, using −500 pA pulses during L_{late} produced the same magnitude of effect as visual sensitization. We conclude that a decrease in inhibition from sustained amacrine cells, when occurring during the baseline condition of a low-contrast stimulus, is sufficient to cause sensitization of the ganglion cell light response.

We then similarly computed whether depolarizing an amacrine cell and thus restoring the level of inhibition during L_{early} would cancel sensitization. We tested whether a single transformation, T_{Both}, fit to simultaneously capture the effects of depolarizing current and the recovery from sensitization could do as well as the two transformations T_{Rec} or T_{Dep} fit separately to capture the recovery from sensitization and current injection, respectively (Figure 4B). We found that the single transformation $\kappa_+ T_{Both}$ with scaling parameter κ_+ captured 90.8% ± 3.3% of the effect of the recovery from sensitization from L_{early} to L_{late} as captured by the single transformation T_{Rec} fit only to capture the recovery from sensitization (Figure 4C). Furthermore, T_{Both} captured 97.1% ± 1.1% of the effects of current that were captured by T_{Dep}, which was fit only to model the effects of current injection (Figure 4C). The value of κ_+ (Figure 4D) was 1.49 ± 0.31, indicating that, on average, the effect of visual sensitization was 1.49 times larger than the effect of +500 pA of current injected into a single amacrine cell during L_{early}. This asymmetry between the magnitude of the effect of hyperpolarization versus depolarization is consistent with the previously reported action of sustained Off amacrine cells working through disinhibition, whereby a nonlinearity in transmission enhances the effect of hyperpolarization and diminishes the effect of depolarization [19].

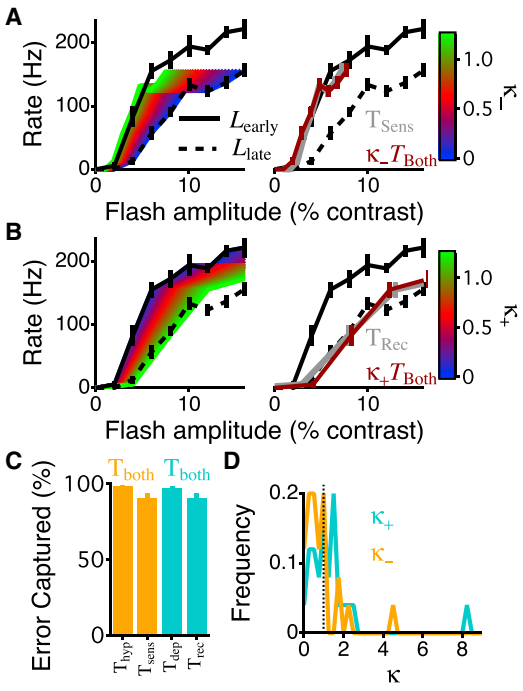

Figure 4. Amacrine Transmission Can Induce or Negate Sensitization

(A) Left: ganglion cell response curves, $G(s)$, from an example cell under control conditions during L_{early}, $G_E(s)$, (solid line) and during L_{late}, $G_L(s)$ (dotted line). Curves in the background are scaled versions of the transformation $\kappa_- T_{Both} = (\kappa_- \mu_{B-}, \kappa_- v_{B-})$ scaled by different values of k. The curve with a value of $\kappa_- = 1$ indicates T_{Both}, the best fit transformation to capture both the change in $G_L(s)$ from sensitization (to $G_E(s)$) and the change in $G_L(s)$from hyperpolarization. Right: same measured control response curves, $G_E(s)$ and $G_L(s)$, along with the L_{late} curve, $G_L(s)$, transformed by two different transformations are shown: T_{Sens} (gray, obscured by the maroon curve) and $\kappa_- T_{Both}$ (maroon), with optimized κ_-.

(B) Left: same as (A) for the transformation $\kappa_+ T_{Both} = (\kappa_+ \mu_{B+}, \kappa_+ v_{B+})$. Right: same as (A) for the transformation T_{Rec} is shown (gray, obscured by the maroon curve), capturing the recovery from sensitization from L_{early} to L_{late} and $\kappa_+ T_{Both}$ (maroon), with optimized κ_+ .

(C) Left: error captured by the simultaneous transformations T_{Both} and $\kappa_- T_{Both}$ as a percentage of the error captured by the separately fit transformations T_{Hyp} and T_{Sens}, respectively. Right: the same for the simultaneous transformations T_{Both} and $\kappa_+ T_{Both}$ and the single transformations T_{Dep} and T_{Rec} is shown.

(D) Histograms of κ values for all pairs of cells that had ganglion cells that sensitized (adaptation index > 0.05) and were 200 μm from each other (n = 25 cell pairs, 19 amacrine cells) for the transformation of the hyperpolarizing curves during L_{late} (κ_-) and depolarizing curves during L_{early} (κ_+). Dashed vertical line indicates $\kappa = 1$, meaning that the effects of current injection and sensitization were the same magnitude.

Error bars in (A)–(C) indicate SEM. See also Figure S3.

Experimentally decreasing inhibition from an amacrine cell during L_{late} produces a ganglion cell light response similar to the sensitized response during L_{early}, and experimentally increasing inhibition from an amacrine cell during L_{early} cancels sensitization, producing a ganglion cell response similar to that during L_{late}. We therefore conclude that decreased inhibition from sustained Off-type amacrine cells, which arises from the observed amacrine hyperpolarization (Figure 2F) and the observed decrease in amacrine transmission during sensitization (Figures 3C, 3E, and 3F), is both necessary for sensitization and sufficient to sensitize the ganglion cell response.

Direct Amacrine Current Injection Can Substitute for Light in Triggering Sensitization

The previous results show that a decrease in amacrine inhibition sensitizes the ganglion cell light response but do not show whether the high-contrast signal in the amacrine cell itself triggers subsequent ganglion cell sensitization. Alternatively, this decrease in amacrine inhibition could arise as a modulatory effect from some other pathway. To test whether the signal within the amacrine cell itself can initiate the process that subsequently sensitizes nearby ganglion cells, we designed an experiment to present a low-contrast visual stimulus while injecting current into an amacrine cell so only that cell experiences high contrast. To mimic the response to a high-contrast visual stimulus, we used a record and playback approach (Figure 5A) [19]. First, we recorded the amacrine response to a high-contrast visual stimulus and then we presented a low-contrast visual stimulus while injecting into the amacrine cell a sequence of current that reproduced the voltage change recorded previously (Figure 2D), while measuring the response of multiple ganglion cells. Thus, we repeated the high- and low-contrast stimulus protocol of Figure 2, except that the high-contrast visual stimulus was replaced with amacrine current injection (Figures 5A and 5B), and the visual stimulus was comprised of exclusively low contrast. Injected current had a SD ranging from 195 to 418 pA (313 ± 62 pA; mean ± SD). Because of the high resistance of sharp microelectrodes, it was difficult to directly measure the voltage change while injecting current. However, by filtering the current with an exponential filter measured by injecting steady current pulses (Figure S2), we estimated that this injected current produced voltage fluctuations in the amacrine cell with a SD of 4.2 ± 0.5 mV, which is similar in magnitude to the response from the high-contrast stimulus (4.0 ± 0.6 mV).

The high-contrast current injected into the amacrine cell was sufficient to induce sensitization in ganglion cells (Figures 5C–5E; p = 0.002; n = 76 ganglion cells, 22 amacrine cells). This effect was specific to nearby ganglion cells, having a space constant of $\lambda = 311 \pm 150\ \mu m$. The spatial decay was comparable to prior measurements of the spatial extent of sensitization in fast Off adapting ganglion cells produced by a localized stimulus (Figure S4). Similar experiments in horizontal cells showed that the signal experienced by horizontal cells did not cause sensitization (Figure 5E).

In addition, visual sensitization generates an afterhyperpolarization as a distinct effect from adaptation of amacrine transmission (Figure 2D). However, current injection did not consistently create an afterhyperpolarization in amacrine cells (Figure 5F). This lack of afterhyperpolarization indicates a dissociation between the two stages of adaptation. A single biophysical site (e.g., spike-dependent conductances in the amacrine cell) is likely not responsible for both adaptation in the visual to amacrine membrane potential stage and the amacrine membrane potential to ganglion cell stage. In summary, the signal experienced by single sustained Off amacrine cells during local high contrast is sufficient to induce a portion of the sensitization experienced by nearby ganglion cells to a low-contrast visual stimulus.

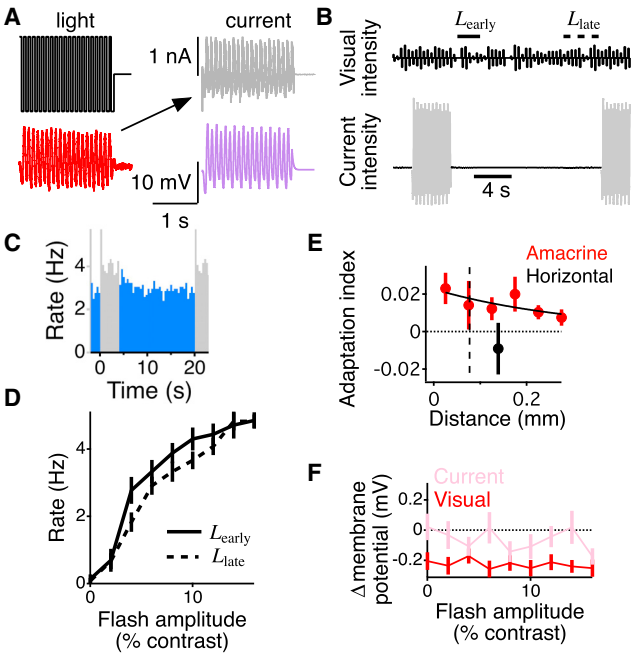

Figure 5. Current Injection into Amacrine Cells Is Sufficient to Induce Sensitization in Ganglion Cells

(A) Schematic of record and playback technique [19] during high-contrast period for example cell in (B). (Left) Visual high-contrast stimulus (top, black) and membrane potential response of amacrine cell (bottom, red). The membrane potential response was then deconvolved with an exponential filter representing the membrane time constant (Figure S2) to yield a current (right, top, gray). This injected current was such that, when convolved with the membrane time constant, it closely approximated the membrane potential response during high contrast (right, bottom, purple). The recorded membrane potential (red) and estimated membrane potential (purple) are plotted on the same scale for comparison.

(B) The visual stimulus was a continuous low contrast composed of 9 different flashes randomly presented (top). Each flash lasted for 400 ms, with 100 ms above the mean, 100 ms below the mean, and 200 ms at the mean intensity. Current was injected into a single amacrine cell to mimic its high-contrast response using a record and playback approach [19] (STAR Methods).

(C) Average response of a ganglion cell to the stimulus protocol in (B). Gray indicates the time of current injection, and the blue color indicates the time without current injection. This ganglion cell had an adaptation index of 0.05 in response to high-contrast current injected into the amacrine cell.

(D) Average response of the ganglion cell in (C) to the 9 different flashes presented in the visual stimulus during L_{early} and L_{late}, as indicated in (B).

(E) Average adaptation index of all recorded fast Off ganglion cells plotted relative to the distance between the ganglion cells and amacrine (red) or horizontal cells (black). Data come from a total of 76 ganglion cells paired with 22 amacrine cells and 10 ganglion cells paired with 3 horizontal cells. Black curve shows an exponential fit to the amacrine cell data.

(F) Average difference in membrane potential between L_{late} and L_{early} for amacrine cells (n = 22) following a visual high contrast (black) or a high-contrast current injected into the amacrine cell (gray). Negative values indicate that the cell was depolarized during L_{late} compared to L_{early}.

Error bars in (D)–(F) indicate SEM. See also Figure S4.

Although recreating the signal produced by high contrast in the single amacrine cell was sufficient to induce measurable sensitization in ganglion cells, sensitization from visual stimulation was 9.1 ± 0.2 times greater. This difference is likely because visual stimulation activates more than a single amacrine cell type, as amacrine cells with more sustained responses are not a single morphological cell type of cell [29]. In addition, if synapses are electrotonically distant from the soma, dynamically varying current injection may activate those synapses less than visual stimulation and less than steady current (Figure 3). Because it appears that current injection produces a membrane potential response that in some cases slightly exceeds a single exponential (Figure S2), this may be evidence of electrotonically distant compartments in the cell, implying that the change in membrane potential at the synapse may be smaller than estimated.

Adapting Inhibitory Transmission in a Model of Sensitization

To quantitatively test whether reduced inhibition from amacrine cells, as shown above, could mediate sensitization, we extended a previous model that uses an adaptive component that represents the properties of synaptic vesicle release [11]. Previous models of sensitization consisted of excitatory and inhibitory pathways, each having a linear temporal filter followed by a threshold nonlinearity [3, 5]. Both pathways adapt, with the output of the inhibitory pathway delivered prior to the threshold of the excitatory pathway. These previous models captured the qualitative aspect of sensitization, in particular, the slow dynamics in firing rate, but did not accurately capture membrane potential fluctuations. Nor were they quantitatively compared with the measured shift in the ganglion cell response curve during sensitization. We retained the same neural pathway structure in the current model, although to generate adaptation in the two pathways, we used a more biophysical, first-order kinetic model of the type used to capture chemical reactions, such as synaptic vesicle recycling (Figure 6A). This type of linear-nonlinear-kinetic (LNK) model accurately captures the membrane potential fluctuations of adapting neurons, as well as all of their adaptive properties [11]. The delivery of the output of the inhibitory pathway to the excitatory pathway prior to its nonlinearity is consistent with presynaptic inhibition onto bipolar cell terminals (Figure 6B), as has been observed in the synaptic terminals of zebrafish during sensitization [4], with the threshold in the excitatory pathway corresponding to the threshold of the voltage-dependent calcium channel [30].

By construction, this model's inhibitory pathway had only a single stage of adaptation, in contrast with our experiments, which showed adaptation in the stage of visual stimulus to amacrine membrane potential and from the stage of amacrine membrane potential to ganglion cell response. In addition, adaptation at the level of the membrane potential was comparatively small, whereas the change in amacrine transmission was comparatively large. Furthermore, our model was not constrained by a fit to amacrine cell data. Thus, we opted to keep a single adaptive stage rather than two less constrained stages.

To initially fit parameters, we first optimized the parameters of the model using an intracellular recording from a sensitizing ganglion cell in response to a uniform field white noise stimulus (Figure 6C). Under these conditions, sustained amacrine cells do not adapt in terms of their light response [24], as opposed to what occurs in response to a spot stimulus (Figures 2D–2F), allowing us to focus on how adaptation in sustained Off amacrine cell transmission (Figure 3) causes sensitization. The continuous

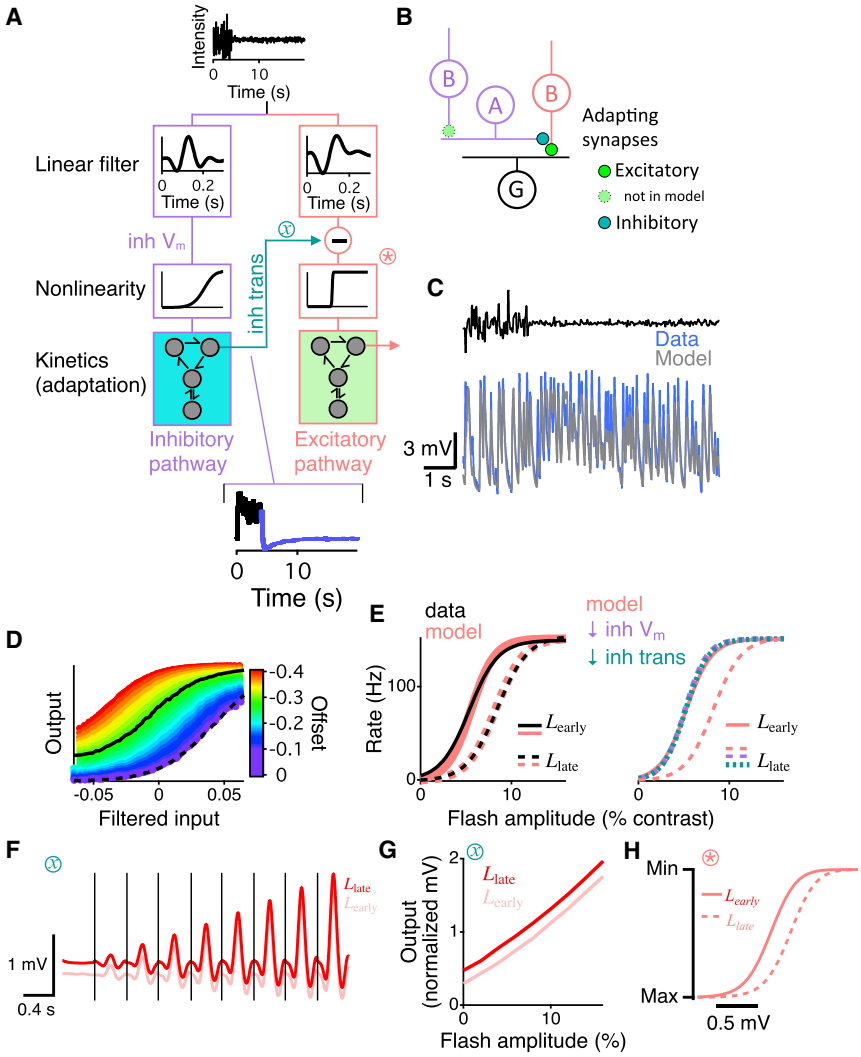

Figure 6. Computational Model of Sensitization Confirms Reduced Inhibition Can Cause Sensitization

(A) Two pathway linear-nonlinear-kinetic (LNK) model [11], each pathway consisting of a linear temporal filter, a static nonlinearity, and a first-order kinetic block (STAR Methods). The inhibitory pathway (left) delivers its output prior to the threshold of the excitatory pathway (right), representing presynaptic inhibition [4, 5]. (Inset) The output of the inhibitory pathway is shown. Blue indicates low contrast.

(B) Schematic of possible circuit implementing sensitization, colored lines and synapses correspond to inhibitory and excitatory pathways in (A). The adapting excitatory synapse in the inhibitory pathway is not represented in the model.

(C) Intracellular recording from a sensitizing ganglion cell responding to uniform field Gaussian white noise at the transition between 35% and 5% contrast, compared to the fit of the model in (A). The membrane depolarization that underlies sensitization is evident after the transition.

(D) The nonlinearity of a linear-nonlinear (LN) model (different from the linear and nonlinear component of the LNK model) at different values of offset for the inhibitory pathway. Solid and dashed lines show the measured nonlinearities of an LN model for L_{early} and L_{late}, respectively.

(E) Left: sigmoidal flash response curves with parameters equal to the median value of the population of cells that sensitized with an adaptation index of >0.05 for L_{early} and L_{late}, compared with the model output when presented with the flash stimuli from Figures 2, 3, 4, and 5. To fit these curves, two parameters of the model were optimized that scaled the output of the inhibitory pathway by a factor as well as the amount of adaptation in the inhibitory pathway. Right: flash response curves of the model in the control condition during L_{early} and L_{late} and when inhibition was reduced during L_{late} either prior to the threshold of the inhibitory pathway or at the output of the pathway (location labeled as inh V_m and inh trans, respectively), in (A) are shown.

(F) Flash responses of the output of the model's inhibitory pathway during L_{early} and L_{late} at the point indicated by the *x* symbol in (A). Responses were scaled in amplitude so that the SD of the 100% contrast flash responses (not shown) were the same for the recorded amacrine cells (Figure 2) and the model. Responses can be compared with data in Figure 2E.

(G) Amplitude of responses in (F) as a function of flash amplitude during L_{early} and L_{late} for comparison with data in Figure 2G.

(H) Nonlinearity in excitatory pathway at point indicated by asterisk symbol in (A). Shown is the relative position during L_{early} and L_{late}, changing as a result of the small steady shift in inhibition. Note that this nonlinearity, a single stage in the model, is different from the nonlinearities shown in (E), which are nonlinearities from a LN model fit to the entire model.

membrane potential provides a greater amount of information to optimize the model, and the white noise stimulus explores a larger range of stimulus space than our flash stimuli used to more precisely quantify the effects of current injection.

This model captured sensitization at the level of the membrane potential, including the millisecond timescale membrane potential fluctuations and the depolarization during L_{early} (Figures 6A–6C). By computing a linear-nonlinear (LN) model fit to the output of the entire model, we confirmed that the threshold of the nonlinearity was lower during L_{early}, indicating that the model was sensitizing (Figure 6D). The two-pathway LNK model then allowed us to assess whether changes in the level of inhibition could mediate the ganglion cell response through sensitization. By decreasing the offset of the inhibitory pathway prior to its inhibiting the excitatory pathway, we could change the ganglion cell response over the range that occurs during sensitization, smoothly changing the nonlinearity of an LN model fit to the two-pathway LNK model (Figure 6D).

To then compare this model to a population of ganglion cells, we adjusted two parameters that controlled (1) the mean level of inhibition and (2) the amount of adaptation in the inhibitory pathway. We found the values of those two parameters that enabled the model to most closely match the median response curves of ganglion cells that exhibited sensitization (Figure 6E). Based on our experimental results from injecting current into amacrine cells, we tested in the model whether reducing the

mean output of the inhibitory pathway could sensitize the overall model. We reduced the mean output of the inhibitory pathway in the model in two ways, either by decreasing the mean value of the inhibitory pathway prior to its internal threshold, corresponding to adaptation of the membrane potential (Figure 2D), or by decreasing the magnitude of the output of the inhibitory pathway, corresponding to adaptation of amacrine transmission (Figures 3C–3G). We found that either manipulation applied to the L_{late} time period could change the L_{late} response curve into one that closely matched the L_{early} response curve (Figure 6E). Thus, the model confirms that sensitization could be caused by a decrease in inhibitory transmission arising from adaptation of the amacrine cell membrane potential and decrease in amacrine transmission.

To gain insight into the necessary magnitude of change in the inhibitory pathway, we compared the final output of the model inhibitory pathway with our amacrine cell recordings. To facilitate this comparison, we normalized the model so that the response to a 100% contrast stimulus had the same SD in the model and in the average amacrine response. During low contrast, the model's inhibitory response was very close in amplitude to the amacrine response. In addition, the model showed a hyperpolarization during L_{early}, without a change in the amplitude of the response compared to L_{late} (Figures 6F and 6G), as we saw in the data (Figures 2E–2G). Finally, the magnitude of the model's hyperpolarization, when put on the same scale as the data, was similar, being 0.17 mV, as compared to 0.24 mV in the data.

This correspondence between the model's inhibition and the amacrine cell response allowed us to ask the question of how a small steady shift in inhibition (Figures 2F–2H) could potentially have a substantial effect on the ganglion cell response. In the model, the only change that produces sensitization is this small, steady shift in inhibitory output. We examined the effect of this shift relative to the slope of the nonlinearity of the excitatory pathway (Figure 6H), which is different from the nonlinearity of a LN model fit to the entire model (Figure 6E). Because the nonlinearity of the excitatory pathway was steep, even though the decrease in inhibition that feeds into this nonlinearity was small, the decrease in inhibition effectively caused a substantial shift in the steep and sensitive excitatory nonlinearity. Thus, although it may be tempting to dismiss the small hyperpolarization of the amacrine membrane potential in favor of the larger, 40% reduction in inhibitory transmission from the amacrine cell, in either case, the high sensitivity of the ganglion cell indicates that a small change in inhibition can have a large effect.

We further compared the time course of the recovery of inhibition and sensitization to see whether the model could explain why the time course of inhibition is slightly longer than that of sensitization (Figure 2I). The model showed a similar relationship between the two processes, with the recovery of inhibition having a time constant of 3.5 s and sensitization of the model output having a faster time constant of 1.5 s. This difference can be explained by the observation that the inhibitory signal crosses the excitatory pathway threshold, as an accelerating nonlinearity will decrease the time constant of a signal, e.g., e^{-t} has a longer time constant than $(e^{-t})^2 = e^{-t/0.5}$. In summary, this computational model captures membrane potential fluctuations and sensitization in ganglion cells using an adapting inhibitory pathway.

DISCUSSION

Here, we have shown, using neural recordings, dynamic perturbations, and computational modeling, that reduced inhibition from sustained amacrine cells mediates sensitization in retinal ganglion cells. A decrease in tonic synaptic transmission from sustained amacrine cells is correlated spatially and temporally with sensitization (Figure 3). This reduction of inhibition is necessary for sensitization and is sufficient to generate sensitization when added to the baseline condition of the retina responding to a low-contrast stimulus (Figure 4).

As a separate conclusion, the visual response of a single amacrine cell is sufficient to trigger a measurable fraction of sensitization (Figure 5), suggesting the model that the reduction in inhibitory transmission arises from visual activation of amacrine cells that causes synaptic depression. Taken together, these results show that a reduction in inhibition from sustained amacrine cells mediates retinal sensitization.

We further observe a small amount of adaptation at the level of the amacrine cell soma membrane potential. It is uncertain how much this hyperpolarization further reduces inhibition during sensitization on top of the ~40% decrease in the synaptic gain that has a large influence on tonic transmission. But because the amacrine cell's soma is an unknown electrotonic distance from the synapse, changes in membrane potential may be larger at the synaptic terminal.

We used a biophysically plausible model [11, 31–33] to confirm that a reduction of inhibition could create sensitization. This model captured both millisecond level fluctuations of the ganglion cell membrane potential as well as sensitization of the firing rate (Figure 6). Because the internal components of the model correspond to synaptic vesicle release [11] and sustained amacrine cell responses (Figure 6), the model supports a mechanistic and functional explanation for the magnitude of the changes seen in the data.

A reduction of inhibition has been shown to underlie elevations of sensitivity in the visual cortex [34] and behavioral choice in *Drosophila* [35], but how these computations unfold within the circuit is unknown. The detailed circuitry for inhibitory transmission is less well known than for excitation, and although the decrease in inhibition that underlies sensitization may derive from synaptic depression of the amacrine cell itself, it may also involve more complex polysynaptic transmission. Thus, our studies reveal a mechanistic contribution from a particular component, the amacrine to ganglion cell stage, and further studies will be needed to further subdivide this stage into smaller mechanistic parts.

Adaptation Arising from Narrow-Field Amacrine Cells

Note that our results indicate that sustained Off amacrine cells mediate some amount of sensitization, which does not rule out whether there are other pathways that also mediate some component of sensitization. In some cases, injection of current pulses caused sensitization greater than that observed from a visual stimulus, whereas in other cases, current pulses caused less than the full observed effect of sensitization (Figure 4D). Furthermore, playing back the response of a white noise visual stimulus into a single amacrine cell caused less than the full amount of sensitization (Figure 5), presumably because more than one amacrine cell is activated by a visual stimulus, implying that more than one amacrine

cell type acts to cause sensitization. Although our strong localized stimulus may activate all amacrine cell types, because our prior studies indicate that the spatial scale of sensitization from a localized stimulus is less than 300 μm [5] (Figure S4), we expect that narrow-field cells mediate most of sensitization from a localized stimulus. It will therefore be important to characterize the number of narrow-field sustained amacrine cell types.

Our estimate of how many other amacrine cell types participate in sensitization may be influenced by the electrotonic distance between the soma and the processes that receive input and deliver output. There may also be an influence of sharp electrode penetration, which can increase the effective electrotonic distance. A large distance may cause our current injection stimuli to have a smaller effect at the synapse than visual stimulation.

Updating of Predictive Sensitization

Sensitization has been proposed to form a prediction of the future location of a moving object, given the expectation that, if an object moves, it will likely be present nearby in the near future [5]. We found that directly manipulating the amacrine cell membrane potential from a single cell during sensitization could cancel most of the effect of sensitization (Figure 4), yet injecting a high-contrast current into the amacrine cell only reproduces a fraction of sensitization (Figure 5). Although this difference could result from differences in experimental conditions in that, in one case, current was applied following a high-contrast visual stimulus, it is worth considering that, under natural conditions, a larger change in steady amacrine cell membrane potential might act to cancel sensitization due to a visual stimulus. If so, a new stimulus effective at depolarizing those amacrine cells could act at an immediate timescale—faster than sensitization—to potentially cancel previously created sensitization. This local cancellation of sensitization might occur even at the level of a single amacrine cell. Thus, given the predictive nature of sensitization to alert the ganglion cell to the potential for new motion of a localized object, a subsequent movement of that object that depolarizes Off-type amacrine cells could serve to cancel previous sensitization, thus both allowing for the response to new motion and acting to sensitize that new location for subsequent stimuli. Further experiments will be required to confirm this hypothesis of local stimuli to dynamically update the state of sensitization.

Sensitization is predictive in ganglion cells that act as feature detectors for stimuli, such as differential motion. For a strong stimulus, detection of a cell's preferred stimulus feature leads to enhanced sensitivity for that feature [5]. Because adaptation and synaptic depression are highly prevalent in the nervous system, a general strategy for prediction may be to control the sensitivity for a feature by using an inhibitory pathway that suppresses that feature, allowing depression of inhibition to generate feature-specific sensitization and thereby enhancing the future sensitivity for that feature. Enhanced sensitivity due to specific decrease in inhibition may therefore underlie sensitization observed in the cortex [36–38] and may reflect a general mechanism for prediction in the nervous system.

Adapting Inhibition May Enable Distinct Sensitizing Components

Although, in principle, sensitization could have been created by synaptic facilitation of excitatory transmission rather than adaptation of inhibition, causing excitatory cells to facilitate would sacrifice the ability to adapt to the changing strength of the primary signal through contrast adaptation [39]. In addition, inhibitory cells are more diverse and thus potentially provide a much richer set of features for which a ganglion cell can elevate its sensitivity. Thus, this arrangement allows a cell to maintain its sensitivity to its primary features and elevate its sensitivity when other features conveyed by inhibitory pathways are more likely to be present.

Because excitation adapts, this adaptation opposes sensitization in the neural pathways that lead to a downstream neuron. Thus, the final result of net sensitization at any one time depends on there being an excess of sensitization over adaptation within those pathways. Under the model that decreasing excitation causes adaptation [11, 12] and decreasing inhibition causes sensitization, net sensitization must arise from differences in the properties of excitatory and inhibitory plasticity. An advantage of generating sensitization by adaptation of inhibitory transmission could be that changes in amacrine transmission can allow sensitization to be generated with flexible dynamics that are distinct from other excitatory plasticity in the circuit, a capability enabled by a diverse inhibitory population.

STAR★METHODS

Detailed methods are provided in the online version of this paper and include the following:

- KEY RESOURCES TABLE
- LEAD CONTACT AND MATERIALS AVAILABILITY
- EXPERIMENTAL MODEL AND SUBJECT DETAILS
- METHOD DETAILS
  - Extracellular recording
  - Intracellular recording
- QUANTIFICATION AND STATISTICAL ANALYSIS
  - Receptive field measurement
  - Measuring changing response curves
  - Scaling parameter for amacrine cell transmission
  - Linear-Nonlinear-Kinetic model
  - Visual stimulation comparison to injected current
- DATA AND CODE AVAILABILITY

SUPPLEMENTAL INFORMATION

Supplemental Information can be found online at https://doi.org/10.1016/j.cub.2019.06.081.

ACKNOWLEDGMENTS

We thank D. Baylor, P. Jadzinsky, F. Zenke, S. Mensi, C. Pozzorini, and F. Dunn for helpful discussions and J. Raymond for commenting on the manuscript. This work was supported by grants from the NEI (R01EY022933 and R01EY025087), Pew Charitable Trusts, McKnight Endowment Fund for Neuroscience, the Alfred P. Sloan Foundation, and the E. Matilda Ziegler Foundation (S.A.B.) and by the Stanford Medical Scientist Training Program, an NSF IGERT graduate fellowship, and an NIH R25 (R25MH060482 to D.B.K.).

AUTHOR CONTRIBUTIONS

D.B.K. and S.A.B. designed the study, D.B.K. performed the experiments, D.B.K. and S.A.B. developed the analyses, D.B.K. and G.P. processed the cells for imaging, Y.O. fit the LNK model, and D.B.K. and S.A.B. wrote the manuscript.

DECLARATION OF INTERESTS

The authors declare no competing interests.

Received: October 3, 2018
Revised: May 14, 2019
Accepted: June 27, 2019
Published: August 1, 2019

REFERENCES

1. Hubel, D.H., and Wiesel, T.N. (1962). Receptive fields, binocular interaction and functional architecture in the cat's visual cortex. J. Physiol. *160*, 106–154.
2. Martinez, L.M. (2011). A new angle on the role of feedfoward inputs in the generation of orientation selectivity in primary visual cortex. J. Physiol. *589*, 2921–2922.
3. Kastner, D.B., and Baccus, S.A. (2011). Coordinated dynamic encoding in the retina using opposing forms of plasticity. Nat. Neurosci. *14*, 1317–1322.
4. Nikolaev, A., Leung, K.-M., Odermatt, B., and Lagnado, L. (2013). Synaptic mechanisms of adaptation and sensitization in the retina. Nat. Neurosci. *16*, 934–941.
5. Kastner, D.B., and Baccus, S.A. (2013). Spatial segregation of adaptation and predictive sensitization in retinal ganglion cells. Neuron *79*, 541–554.
6. Montague, P.R., and Sejnowski, T.J. (1994). The predictive brain: temporal coincidence and temporal order in synaptic learning mechanisms. Learn. Mem. *1*, 1–33.
7. Schultz, W., Dayan, P., and Montague, P.R. (1997). A neural substrate of prediction and reward. Science *275*, 1593–1599.
8. Sanes, J.R., and Lichtman, J.W. (1999). Can molecules explain long-term potentiation? Nat. Neurosci. *2*, 597–604.
9. Cook, P.B., Lukasiewicz, P.D., and McReynolds, J.S. (2000). GABA(C) receptors control adaptive changes in a glycinergic inhibitory pathway in salamander retina. J. Neurosci. *20*, 806–812.
10. Dale, N., Schacher, S., and Kandel, E.R. (1988). Long-term facilitation in Aplysia involves increase in transmitter release. Science *239*, 282–285.
11. Ozuysal, Y., and Baccus, S.A. (2012). Linking the computational structure of variance adaptation to biophysical mechanisms. Neuron *73*, 1002–1015.
12. Jarsky, T., Cembrowski, M., Logan, S.M., Kath, W.L., Riecke, H., Demb, J.B., and Singer, J.H. (2011). A synaptic mechanism for retinal adaptation to luminance and contrast. J. Neurosci. *31*, 11003–11015.
13. Berry, M.J., 2nd, Brivanlou, I.H., Jordan, T.A., and Meister, M. (1999). Anticipation of moving stimuli by the retina. Nature *398*, 334–338.
14. Hosoya, T., Baccus, S.A., and Meister, M. (2005). Dynamic predictive coding by the retina. Nature *436*, 71–77.
15. Schwartz, G., Taylor, S., Fisher, C., Harris, R., and Berry, M.J., 2nd. (2007). Synchronized firing among retinal ganglion cells signals motion reversal. Neuron *55*, 958–969.
16. Schwartz, G., Harris, R., Shrom, D., and Berry, M.J., 2nd. (2007). Detection and prediction of periodic patterns by the retina. Nat. Neurosci. *10*, 552–554.
17. Palmer, S.E., Marre, O., Berry, M.J., 2nd, and Bialek, W. (2015). Predictive information in a sensory population. Proc. Natl. Acad. Sci. USA *112*, 6908–6913.
18. Zhang, A.-J., and Wu, S.M. (2010). Responses and receptive fields of amacrine cells and ganglion cells in the salamander retina. Vision Res. *50*, 614–622.
19. Manu, M., and Baccus, S.A. (2011). Disinhibitory gating of retinal output by transmission from an amacrine cell. Proc. Natl. Acad. Sci. USA *108*, 18447–18452.
20. de Vries, S.E.J., Baccus, S.A., and Meister, M. (2011). The projective field of a retinal amacrine cell. J. Neurosci. *31*, 8595–8604.
21. Cook, P.B., Lukasiewicz, P.D., and McReynolds, J.S. (1998). Action potentials are required for the lateral transmission of glycinergic transient inhibition in the amphibian retina. J. Neurosci. *18*, 2301–2308.
22. Baccus, S.A., Olveczky, B.P., Manu, M., and Meister, M. (2008). A retinal circuit that computes object motion. J. Neurosci. *28*, 6807–6817.
23. Lehky, S.R., and Sejnowski, T.J. (1988). Network model of shape-from-shading: neural function arises from both receptive and projective fields. Nature *333*, 452–454.
24. Baccus, S.A., and Meister, M. (2002). Fast and slow contrast adaptation in retinal circuitry. Neuron *36*, 909–919.
25. Yang, C.-Y., Lukasiewicz, P., Maguire, G., Werblin, F.S., and Yazulla, S. (1991). Amacrine cells in the tiger salamander retina: morphology, physiology, and neurotransmitter identification. J. Comp. Neurol. *312*, 19–32.
26. Carandini, M., and Ferster, D. (1997). A tonic hyperpolarization underlying contrast adaptation in cat visual cortex. Science *276*, 949–952.
27. Manookin, M.B., and Demb, J.B. (2006). Presynaptic mechanism for slow contrast adaptation in mammalian retinal ganglion cells. Neuron *50*, 453–464.
28. Sagdullaev, B.T., Eggers, E.D., Purgert, R., and Lukasiewicz, P.D. (2011). Nonlinear interactions between excitatory and inhibitory retinal synapses control visual output. J. Neurosci. *31*, 15102–15112.
29. Pang, J.J., Gao, F., and Wu, S.M. (2002). Segregation and integration of visual channels: layer-by-layer computation of ON-OFF signals by amacrine cell dendrites. J. Neurosci. *22*, 4693–4701.
30. Mennerick, S., and Matthews, G. (1996). Ultrafast exocytosis elicited by calcium current in synaptic terminals of retinal bipolar neurons. Neuron *17*, 1241–1249.
31. Mongillo, G., Barak, O., and Tsodyks, M. (2008). Synaptic theory of working memory. Science *319*, 1543–1546.
32. Mensi, S., Hagens, O., Gerstner, W., and Pozzorini, C. (2016). Enhanced sensitivity to rapid input fluctuations by nonlinear threshold dynamics in neocortical pyramidal neurons. PLoS Comput. Biol. *12*, e1004761.
33. Kastner, D.B., Schwalger, T., Ziegler, L., and Gerstner, W. (2016). A model of synaptic reconsolidation. Front. Neurosci. *10*, 206.
34. Fu, Y., Tucciarone, J.M., Espinosa, J.S., Sheng, N., Darcy, D.P., Nicoll, R.A., Huang, Z.J., and Stryker, M.P. (2014). A cortical circuit for gain control by behavioral state. Cell *156*, 1139–1152.
35. Jovanic, T., Schneider-Mizell, C.M., Shao, M., Masson, J.-B., Denisov, G., Fetter, R.D., Mensh, B.D., Truman, J.W., Cardona, A., and Zlatic, M. (2016). Competitive disinhibition mediates behavioral choice and sequences in Drosophila. Cell *167*, 858–870.e19.
36. Cohen-Kashi Malina, K., Jubran, M., Katz, Y., and Lampl, I. (2013). Imbalance between excitation and inhibition in the somatosensory cortex produces postadaptation facilitation. J. Neurosci. *33*, 8463–8471.
37. Ganmor, E., Katz, Y., and Lampl, I. (2010). Intensity-dependent adaptation of cortical and thalamic neurons is controlled by brainstem circuits of the sensory pathway. Neuron *66*, 273–286.
38. Mohar, B., Katz, Y., and Lampl, I. (2013). Opposite adaptive processing of stimulus intensity in two major nuclei of the somatosensory brainstem. J. Neurosci. *33*, 15394–15400.
39. Demb, J.B. (2008). Functional circuitry of visual adaptation in the retina. J. Physiol. *586*, 4377–4384.
40. Brainard, D.H. (1997). The psychophysics toolbox. Spat. Vis. *10*, 433–436.
41. Pelli, D.G. (1997). The VideoToolbox software for visual psychophysics: transforming numbers into movies. Spat. Vis. *10*, 437–442.
42. Chichilnisky, E.J. (2001). A simple white noise analysis of neuronal light responses. Network *12*, 199–213.
43. Brenner, N., Bialek, W., and de Ruyter van Steveninck, R. (2000). Adaptive rescaling maximizes information transmission. Neuron *26*, 695–702.

STAR★METHODS

KEY RESOURCES TABLE

REAGENT or RESOURCE	SOURCE	IDENTIFIER
Chemicals, Peptides, and Recombinant Proteins		
Sodium Chloride	Fisher	S271-500
Potassium Chloride	Fisher	P217-500
Calcium Chloride	Fisher	C69-500
Magnesium Chloride	Fisher	M33-500
Sodium Bicarbonate	Fisher	S233-500
D-Glucose	Fisher	D16-500
Neurobiotin	Vector Labs	SP-1120
Streptavidin Alexa Fluor 488	Invitrogen	S1123
Experimental Models: Organisms/Strains		
Larval Tiger Salamander	Wadelco, TX	N/A
Software and Algorithms		
Igor	Wavemetrics	Igor 5, 6, 7
MATLAB	Mathworks	N/A

LEAD CONTACT AND MATERIALS AVAILABILITY

Further information and requests for resources and reagents should be directed to and will be fulfilled by the Lead Contact, Stephen Baccus (baccus@stanford.edu).

This study did not generate new unique reagents.

EXPERIMENTAL MODEL AND SUBJECT DETAILS

Larval tiger salamanders, of either sex, were housed in a cold room at 4°C. All experiments were performed according to procedures approved by the Stanford University Administrative Panel on Laboratory Animal Care.

METHOD DETAILS

Extracellular recording

Retinal ganglion cells were recorded using an array of 60 electrodes (Multichannel Systems) as described [3]. A video monitor projected the visual stimuli at 30 Hz controlled by MATLAB (Mathworks), using Psychophysics Toolbox [40, 41]. Stimuli had a mean intensity of 10 mW/m^2 that was kept constant across stimulus conditions.

Intracellular recording

Simultaneous intracellular and multielectrode recordings from the isolated intact salamander retina were performed as described [19]. Sustained amacrine and horizontal cells were identified by their flash response and their spatiotemporal receptive fields (Figures 2B and S1A), with horizontal cells lacking an inhibitory surround and being greater than 300 μm in diameter. The average membrane potential of sustained amacrine cells was −33.2 ± 2.3 mV, and for horizontal cells was −26.8 ± 7.4 mV. For some of the cells we confirmed that they were in fact amacrine cells by filling and imaging them (n = 4) (Figure S1B). We recorded a total of 33 amacrine cells; however, not all of the amacrine cell recordings were used for all stimulus protocols. We note in the figures and text how many amacrine cells, and paired ganglion cells when appropriate, contributed to each figure.

The output of the ganglion cell response functions for the transmission experiments (Figures 3 and 4) was determined as the maximal firing rate in a 50 ms window averaged across all trials for each flash amplitude. All fast Off ganglion cells that responded in the control conditions (Figure 3B) with an average response over 11 Hz were included in the analysis to determine the changes in the transmission (Figures 3 and 4).

The record and playback experiments (Figure 5) were carried out as previously described [19]. Briefly, the response of an amacrine cell to a visual stimulus was recorded. Then the visual response during high contrast was deconvolved with an exponential filter, capturing the membrane time constant, to create the current necessary to inject to playback the response of the amacrine cell to

high contrast. The injected current was scaled according to the amplitude of the measured membrane potential response, and had a standard deviation ranging from 195 - 418 pA.

QUANTIFICATION AND STATISTICAL ANALYSIS

Statistical analyses are reported with p values in the text. Statistical parameters are cited in the text and the figure legends.

Receptive field measurement

Spatiotemporal receptive fields were measured in one or two dimensions by the standard method of reverse correlation [42] of the spiking response with a visual stimulus consisting of squares that were drawn from a binary distribution, or lines drawn from a Gaussian white noise distribution, such that

$$F(x,y,\tau) = \int_0^T s(x,y,t-\tau)r(t)dt, \qquad \text{(Equation 1)}$$

where $F(x,y,\tau)$ is the linear response filter at position (x,y) and delay τ, $s(x,y,t)$ is the stimulus intensity at position (x,y) and time t, normalized to zero mean, $r(t)$ is the firing rate of a ganglion cell or the membrane potential of an amacrine cell, and $T$is the duration of the recording.

For all amacrine cell recordings, the receptive field of the amacrine cell was measured online, and the stimulus was centered onto the receptive field of the amacrine cell. The distance between an amacrine and ganglion cell was determined as the distance between the centers of two-dimensional Gaussian fits to their receptive fields.

Measuring changing response curves

During high contrast the amplitude of the flash flickered with a period of 200 ms and 100% Michelson contrast, defined as $(I_{max} - I_{min})/(I_{max} + I_{min})$. During low contrast the contrast amplitude of the flash varied randomly every 400 ms and was one of nine values that ranged from 0 – 16% contrast. Changing the distribution of amplitudes slower than the integration time of ganglion cells allowed for a rapid measurement of the ganglion cell response function without having to also measure the ganglion cell temporal filter [43]. Synchronized to the visual stimulus, we injected, randomly interleaved, hyperpolarizing or depolarizing current pulses into the amacrine cell. We computed response curves that were a function of the visual stimulus during L_{early}, $G_E(s)$, as a control, $G_{E+}(s)$ using depolarizing current, and $G_{E-}(s)$ using hyperpolarizing current, and similarly, $G_L(s)$, $G_{L+}(s)$, and $G_{L-}(s)$ during L_{late} (Figures 3A and 3B).

We examined the effect of amacrine cell current on the control ganglion cell light response during L_{late}, $G_L(s)$, which approximated the steady state low contrast response. The response curves under different stimulus conditions were approximately sigmoidal but with different slopes and midpoints, suggesting that one curve could be transformed into another by four parameters that shifted and scaled the response curve horizontally or vertically, or both. Therefore, we captured the transformation caused by amacrine current with manipulations to $G_L(s)$ reflecting changes in four parameters. The two parameters that horizontally shifted and scaled were μ, which shifted $G_L(s)$ with respect to the visual stimulus s, and v, which scaled $G_L(s)$ horizontally with respect to s. These two parameters changed the threshold and slope of $G_L(s)$. The two parameters that vertically shifted and scaled the curve were α, which shifted the output vertically, and β, which scaled the output. These two parameters change the minimal and maximal output of the response function (Figure S3A).

Previously it was concluded that current injection into sustained Off amacrine cells changed the fast Off ganglion cell light response consistent with a presynaptic effect delivered prior to the sharp threshold at the bipolar cell terminal [19]. Therefore, we measured how much of the effect of the current could be captured by only using the input parameters, μ and v for the transformation, compared to using all four parameters. As an example using the depolarizing current condition: for the transformation using all four parameters, $T_{4Dep} = (\mu_{+I}, v_{+I}, \alpha_{+I}, \beta_{+I})$, this was computed by finding the parameters that minimized the difference between $G_L(s)$ and $\beta G_{L+}(e^v s + \mu) + \alpha$. Whereas, for the transformation that only manipulated the input parameters, $T_{4Dep} = (\mu_{+I}, v_{+I})$, we sought to find the values that minimized the difference between $G_L(s)$ and $G_{L+}(e^v s + \mu)$. The multiplicative scaling parameter v was raised to an exponent so that cells would exert their multiplicative effects independently, i.e., one amacrine cell acting with a scaling parameter of v would scale the stimulus by e^v, and two cells would scale the stimulus by e^{2v}.

For hyperpolarizing current during L_{early}, which changed the response curve from $G_L(s)$ to $G_{L-}(s)$, the two parameters of the transformation $T_{Hyp} = (\mu_{-I}, v_{-I})$ accounted for 79.9 ± 3.2% of the total effect of current injection, determined by using the transformation T_{4Hyp}. In solving for T_{Hyp}, we constrained μ and v to be positive. For depolarizing current, which changed the response curve from $G_L(s)$ to $G_{L+}(s)$, the transformation T_{Dep} accounted for 82.3 ± 3.2% of the total effect of current injection, T_{4Dep}. For the transformation T_{Dep}, we constrained μ and v to be negative. Therefore, a transformation of the input dependence of the light response captures most of the effect of current injection, consistent with current injection predominantly working through an effect on the bipolar cell terminal, presynaptic to fast Off-type ganglion cells (n = 60 cell pairs, 24 amacrine cells).

We also measured how much of sensitization could be captured by only the two parameters of the transformation $T_{Sens} = (\mu_S, v_S)$. For sensitization, which changes the light response from $G_L(s)$ during L_{late} to $G_E(s)$ during L_{early}, a horizontal shifting and scaling by

T_{Sens} accounted for 83.2 ± 2.8% of the total effect of sensitization, found using $T_{4Sens} = (\mu_S, \nu_S, \alpha_S, \beta_S)$. For the recovery from sensitization, changing $G_E(s)$ to $G_L(s)$ using only a horizontal shifting and scaling, T_{Sens}, accounted for 87.8 ± 2.0% of the total effect of recovery from sensitization. Thus, most of the effect of sensitization was also captured by a horizontal shifting and scaling of the light response, consistent with a presynaptic effect (n = 43 cell pairs, 23 amacrine cells).

All ganglion response curves were fit using a sigmoid function:

$$y(x) = y_0 \frac{m}{1 + \exp\left(\frac{x_{1/2} - x}{r}\right)}, \quad \text{(Equation 2)}$$

where $m + y_0$ is the maximum value, $x_{1/2}$ is the x value at which the function equals half the distance between the maximum value and y_0, and r controls the rate at which the function increases. The curves were not extrapolated beyond the data limits. The error metric was the root mean squared (rms) difference between the sigmoid fits of the measured response function and the transformed response function. The fraction of the response that was captured by a two-parameter transformation T_2 versus the T_4 transformation was computed as $(E_{T_2} - E_{T_4}/E_0 - E_{T_4})$; where E_{T_2} and E_{T_4} were the errors remaining after the T_2 and T_4 transformations, respectively, and E_0 is the rms difference between the curves without any manipulation.

Scaling parameter for amacrine cell transmission

To account for the effects of multiple amacrine cells and the fact that the effect of current injection on a single cell may differ in magnitude from the effect of sensitization, we computed for the effect of current injection the parameter μ that horizontally shifted the ganglion cell response curve, and the parameter v that horizontally scaled the ganglion cell response curve, $G(e^{\nu}s + \mu)$ to transform the ganglion cell response curve during the control condition onto the response curve under current injection, yielding the transformation $T_{\text{Hyp}} = (\mu_{-I}, \nu_{-I})$ for the transformation of the control curve, $G_L(s)$, onto the hyperpolarized curve, $G_{L-}(s)$, during L_{late}. For comparison, we computed the effects of sensitization between $G_L(s)$ during L_{late} and $G_E(s)$ during L_{early} as the transformation $T_{\text{Sens}} = (\mu_s, \nu_s)$. We then fit all parameters, $(\mu_{B-}, \nu_{B-}, \kappa)$, together so that the transformation $T_{\text{Both}} = (\mu_{B-}, \nu_{B-})$ would most closely match the effects of current by transforming $G_L(s)$ to approximate $G_{L-}(s)$ and so that the scaled transformation $\kappa_- T_{\text{Both}} = (\kappa_- \mu_{B-}, \kappa_- \nu_{B-})$ would most closely match the effects of sensitization by transforming $G_L(s)$ to approximate $G_E(s)$. The same was done for the comparison of $\kappa_- T_{\text{Both}}$, T_{Rec} and T_{Dep}. The fraction of error captured by the single transformation T_{Both} compared to the transformation T_{Sens} was measured as $((E_0 - E_{T_{\text{Sens}}}) - (E_0 - E_{T_B})/E_0 - E_{T_{\text{Sens}}} = E_{T_{\text{B}}} - E_{T_{\text{Sens}}}/E_0 - E_{T_{\text{Sens}}})$; where $E_{T_{\text{B}}}$ is the error for T_{Both}, $E_{T_{\text{Sens}}}$ is the errors for T_{Sens}, and $E_{T_{\text{B}}0}$ is the rms difference between the $G_L(s)$ and $G_E(s)$ curves without any manipulation. The fraction of error captured by T_{Both} compared to the transformations T_{Hyp}, T_{Rec} and T_{Dep} was similarly computed.

Linear-Nonlinear-Kinetic model

The LNK model consisted of two pathways, each consisting of a linear temporal filter $F_{LNK}(t)$, a static nonlinearity, $N(g)$ and a first order kinetic system defined by a transition matrix $\mathbf{Q}(u)$. This model is similar to a two-pathway LNK model described previously [11], and summarized here, with the exception that the output of the first inhibitory pathway was joined with the second excitatory pathway prior to the threshold. The components were parameterized as described below, and all parameters were fit together using a constrained optimization algorithm. For each pathway, the stimulus, $s(t)$, was passed through a linear temporal filter, $F_{LNK}(t)$ and a static nonlinearity, $N(g)$,

$$u(t) = N\left(\int F_{LNK}(t - \tau) s(\tau) d\tau\right) \quad \text{(Equation 3)}$$

Although these two initial stages have the same structure as the linear-nonlinear (LN) model, the filter and nonlinearity are different functions than those computed for an LN model, and are optimized, rather than computed using reverse correlation. The kinetics block of the model was a Markov process defined by

$$\frac{d\mathbf{P}^{\mathsf{T}}(t)}{dt} = \mathbf{P}^{\mathsf{T}}(t)\mathbf{Q}(u), \quad \text{(Equation 4)}$$

where $\mathbf{P}(t)$ is a column vector of m fractional state occupancies such that $\sum_i P_i = 1$, and $\mathbf{Q}$ is an $m \times m$ transition matrix containing the rate constants Q_{ij} that control the transitions between states i and j, with $Q_{ii} = -\sum_{i \neq j} Q_{ij}$. After this differential equation was solved numerically, the output of the model, $r'(t)$ was equal to one of the state occupancies scaled to a response in millivolts,

$$r'(t) = P_2(t)c + d, \quad \text{(Equation 5)}$$

where c and d are a scaling and offset term for the entire recording.

States and rate constants were defined as,

$$\begin{array}{llll} P_1 = R & \text{Resting} & R \rightarrow A: & Q_{12} = u(t)k_a \quad \text{Activation} \\ P_2 = A & \text{Active} & A \rightarrow I_1: & Q_{23} = k_{fi} \quad \text{Fast inactivation} \\ P_3 = I_1 & \text{Inactivated} & I_1 \rightarrow R: & Q_{31} = k_{fr} \quad \text{Fast recovery} \\ P_4 = I_2 & \text{Inactivated} & I_1 \rightarrow I_2: & Q_{34} = k_{si} \quad \text{Slow inactivation} \\ & & I_2 \rightarrow I_1: & Q_{43} = u(t)k_{sr} \quad \text{Slow recovery} \end{array} \qquad \text{(Equation 6)}$$

The change in state occupancy was thus determined as

$$\frac{d\mathbf{P}^{\mathrm{T}}(t)}{dt} = \begin{pmatrix} \dot{P}_1(t) \\ \dot{P}_2(t) \\ \dot{P}_3(t) \\ \dot{P}_4(t) \end{pmatrix} = \mathbf{P}^{\mathrm{T}} \begin{pmatrix} -u(t)k_a & u(t)k_a & 0 & 0 \\ 0 & -k_{fi} & k_{fi} & 0 \\ k_{fr} & 0 & -(k_{fr}+k_{si}) & 0 \\ 0 & 0 & u(t)k_{sr} & -u(t)k_{sr} \end{pmatrix}. \qquad \text{(Equation 7)}$$

A more complex model with an additional adapting stage in the inhibitory pathway representing bipolar cell inputs to the amacrine cell would be needed capture the two-stage adaptation in the inhibitory pathway seen for a localized stimulus. This model for a spatio-temporal stimulus would require many additional parameters for spatiotemporal filters for a population of amacrine cells and an additional adaptive stage, and thus would not be well constrained with current measurements.

The model optimized first to the membrane potential of a ganglion cell in response to a uniform field Gaussian white noise stimulus lasting 300 s that changed in contrast every 20 s [11]. This stimulus allowed an initial optimization of all parameters because it explored a wide range of stimulus sequences. To then account for the responses to a flashing visual spot, two additional parameters were optimized to match the model most closely to the median response curves during L_{early} and L_{late} of the ganglion cell population that exhibited sensitization. Because the total amount of inhibition is expected to be different for a strong localized stimulus than for a uniform stimulus, the constant that scales the entire output of the inhibitory pathway was adjusted. In addition, the slow recovery rate constant was adjusted to control the amount of adaptation in the inhibitory pathway, and thus the overall amount of sensitization in the model.

Visual stimulation comparison to injected current

To compare sensitization deriving from either visual stimulation or injected current, we performed a bootstrap analysis, where we sampled with replacement from the 57 ganglion cells that sensitized to the high contrast visual stimulations (i.e., Adaptation Index > 0) and for which we also had responses in those ganglion cells to the high contrast current injection into an amacrine cell. For each resampling we found the shifting along the x axis that minimized the difference between the L_{early} and L_{late} curves and took the average ratio of that scaling between visual high contrast stimulation and current injection.

DATA AND CODE AVAILABILITY

The data supporting the current study have not been deposited in a public repository because of the nonstandard data format used with our custom acquisition software, but are available from the lead contact (baccus@stanford.edu) on request.

Current Biology, Volume *29*

Supplemental Information

Adaptation of Inhibition Mediates Retinal Sensitization

David B. Kastner, Yusuf Ozuysal, Georgia Panagiotakos, and Stephen A. Baccus

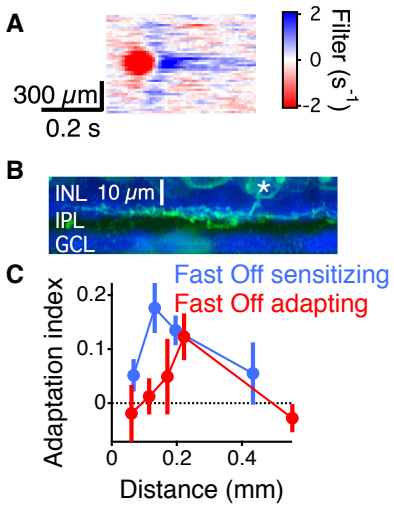

Figure S1. **Amacrine cell identification, related to Figure 2. (A)** Spatiotemporal receptive field of an amacrine cell. Stimulus intensities are indicated by the color scale, with red indicating an intensity below the mean value. **(B)** Image of the dye-filled amacrine cell from **A**. INL is the inner nuclear layer, IPL is the inner plexiform layer, and GCL is the ganglion cell layer. White star indicates the location of the cell body of the filled cell. **(C)** Adaptation Index as a function of distance between fast Off adapting (n = 67) and fast Off sensitizing (n = 28) ganglion cells and the center of the high contrast spot. The ganglion cells in this study reproduced the center-surround adaptive field previously reported, with comparable levels of sensitization [S1].

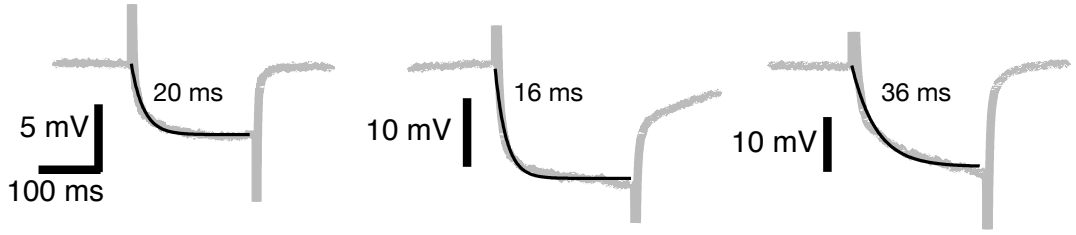

Figure S2. **Effects of current injection in sustained amacrine cells, related to Figure 3.** Shown are responses to hyperpolarizing pulses of -500 pA to three sustained amacrine cells. Responses were fit by a double exponential, yielding one exponential with a time constant < 1 ms created by the sharp microelectrode, and one longer exponential (black curve) that reflected the membrane time constant. Traces were adjusted to eliminate the vertical offset created by the short time constant decay of the electrode. Left cell is the same cell in (Figure 3 B, C).

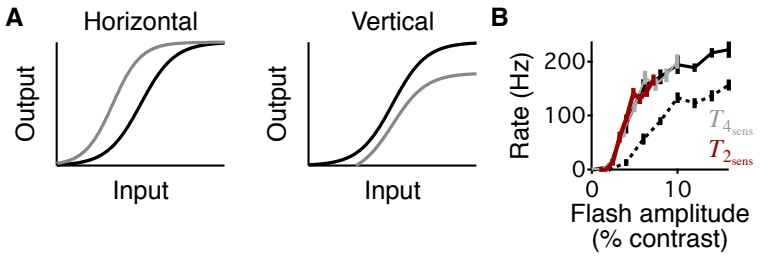

Figure S3. **Amacrine current effects on the ganglion cell response function, related to Figure 4.** **(A)** Example transformation using only a horizontal axis shifting and scaling parameters (left) and using only the vertical axis shifting and scaling parameters (right). **(B)** Same cell as in Figure 3B, with two transformations of L_{late} onto L_{early}. The first transformation, uses all 4 parameters (grey, obscured by maroon line), while the second transformation only uses the horizontal axis parameters (see STAR Methods).

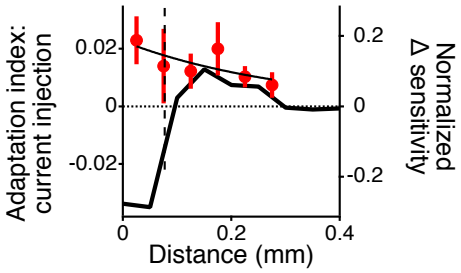

Figure S4. Current induced sensitization decays over a similar spatial scale as the sensitizing surround under a visual stimulus, related to Figure 5. Red points are the same data as plotted in Figure 5D and the black curve is the single cell change in visual sensitivity of fast Off adapting cells generated by a high contrast spot whose boundary is indicated by the dashed vertical line, data reproduced from [S1]. The change in sensitivity from a visual stimulus is negative showing adaptation in the region of the localized adapting high contrast stimulus, and positive showing sensitization outside of the region of the high contrast stimulus.

Supplemental Reference

S1. Kastner DB, Baccus SA (2013) Spatial segregation of adaptation and predictive sensitization in retinal ganglion cells. Neuron 79, 541–554.